Characterization of Birefringent Titanium-Oxide Thin Films Deposited by DC Sputtering

H. P. de Araújo[1,2] and S. G. dos Santos Filho[2]

[1]LSI-TEC – R. Paes Leme, 524 – Ed. Passarelli, cj. 95/96 – Pinheiros, São Paulo / SP, Brazil – CEP: 05424-904
[2]LSI/PSI/EPUSP – Av. Prof. Luciano Gualberto, 158 – trav. 3, Cid. Universitária, São Paulo, SP, Brazil

Abstract — **This work presents the characterization of birefringent properties of titanium-oxide thin films using spectrophotometry and double-cavity Fabry-Perot structures. All films were deposited by DC sputtering over tilted substrates and the birefringence was characterized as a function of the deposition angle by the numerical difference between the refractive indexes for *s*- and *p*-polarized light beams. As a result, the highest value of birefringence (0.03) was obtained for samples tilted at 21º (having the normal axis as reference). A polarizing narrow-band Fabry-Perot filter centered at 400 and 700nm was designed by means of numerical simulations of the multilayer structures using a MATLAB© toolbox to solve the classical optical equations. Using this designed double-cavity Fabry-Perot structure [Ag(40nm) / TiO_2(160nm) / Ag(40nm) / TiO_2(164nm) / Ag(40nm)], transmittance ratios (T_p/T_s) for *p*- and *s*-polarized light beams resulted 1.70 at a wavelength of 699nm and 1.36 at another wavelength of 393nm (centers of the two narrow-band peaks), which corroborated the birefringent characteristics of the nearly-stoichiometric titania (TiO_2) thin films.**

Keywords — Birefringence, DC Sputtering, Titania, Titanium Oxide, TiO_2, Refractive Index.

I. Introduction

There are many potential applications of birefringent layers in nano-optical technologies including integrated optics and polarization-difference imaging (PDI) devices [1-4]. Birefringence or double refraction is an optical property of certain transparent materials, defined as the numerical difference between the refractive indexes for *s*- and *p*-polarized light beams [5]. Titania (TiO_2) thin films can present birefringent properties when they have a obliquely-oriented columnar structure on the surface where they are deposited by e-beam evaporation [5]. The oblique orientation is changed by tilting the substrates relatively to the titanium evaporation source at low partial pressure of oxygen [5]. In this case, a biaxial-like birefringence model, namely *form birefringence*, is normally used for these dielectric films deposited obliquely because they behave like orthorhombic crystals [5].

The Fabry-Perot structure is a device that makes use of interference phenomena due to waves successively reflected between two thinly silvered planes set accurately parallel. This structure has been used for a wide range of applications in metrology and spectroscopy including size measurement and wavelength comparison [5]. Specifically, the two-cavity Fabry-Perot structure using transparent materials with different birefringent materials interposed by thin silver films allows one to filter s- or p-polarized light beams at a very narrow wavelength band [5].

On the other hand, other deposition techniques, including "sputtering", can be used in order to obtain titania thin films with columnar structure [7,8]. Based on the SZM (Structure Zone Models) diagram [7,8], DC sputtered films can present columnar structure for low substrate temperature, moderate substrate voltage and low gas pressure. Although columnar structure can be obtained for sputtered films, there is lack of researching for obliquely-oriented columnar structures using sputtering.

This work presents the first characterization study of birefringent titanium-oxide thin films deposited by DC sputtering over tilted substrates. Besides spectrophotometry, double-cavity Fabry-Perot structures were also used to characterize the birefringent properties.

II. Simulations and Experimental Procedures

For all experiments, thin square sheets of ordinary glass, 0.2mm thick and 25x25mm in size, were used. Titanium oxide deposition was carried out in a DC sputtering equipment using a titanium target (99.999%) in an oxygen partial pressure of 4.10^{-4} Bar. Also, a silver target was available in the same equipment, so it was possible to deposit both materials, sequentially, without the need to open the chamber and break the vacuum. The only exception was to turn the samples by 90° in order to get *p* and *s* materials (90° rotated TiO_x). In this case, the vacuum was broken just after the deposition of the oxide layer, so avoiding to expose the Ag layers to the oxygen at the atmosphere. Another precaution was to start depositing a thin layer of Ti (Ti *flash*) before releasing the oxygen, so avoiding an exposition of the Ag film and preventing its oxidation. Three different inclinations of the substrate were used as schematically shown in figure 1: 21.0°, 28.0° and 32.5°. These angles were measured having the normal axis as reference on the substrate surface.

DC sputtering over the tilted glass plates was performed with sputtering voltage of 1.62kV and sputtering current of 0.6A. The sputtering time was controlled in order to obtain film thickness of approximately 80, 120 or 160nm. Two kinds of samples were prepared: (a) titanium oxide was deposited onto the glass sheets in order to proceed with the spectrophotometry analysis and (b) double-cavity Fabry-Perot structures [Ag(40nm) / TiO_2(160nm) / Ag(80nm) / TiO_2(164nm) / Ag(40nm)] were manufactured using two different targets (Ti and Ag) in order to measure the

transmittance ratio (T_p/T_s). After obtaining the first cavity between two layers of silver, the samples were rotated, or not, around the normal axis by 90° and the second cavity was deposited for each inclination angle shown in figure 1. This structure of the figure 1 with the 90°-rotated cavity was named here as the FP1 device. This device is based on the biaxial-like birefringence model for obliquely-oriented columnar deposition [4]. In this case, the difference between cavity birefringent materials is the highest possible if the sample is rotated by 90° before deposition of the second cavity. In addition, the structure without the 90° rotation was also manufactured and was named here as the FP2 device. In this device, the transmittance ratio (T_p/T_s) is unitary and it is expected just a drift on the narrow-band peak wavelength when the light polarization is changed from "*p*" to "*s*" or vice-versa, due to different optical paths (OP) in the double-cavity Fabry-Perot structure (OP = $n_1 d_1 + n_2 d_2$ where d_1 and d_2 are the cavity thicknesses, n_1 and n_2 are the cavity refractive indexes that vary for *s*- or *p*-polarized light and Ag interlayers are not supposed to influence). These conditions are analyzed in the results and discussion.
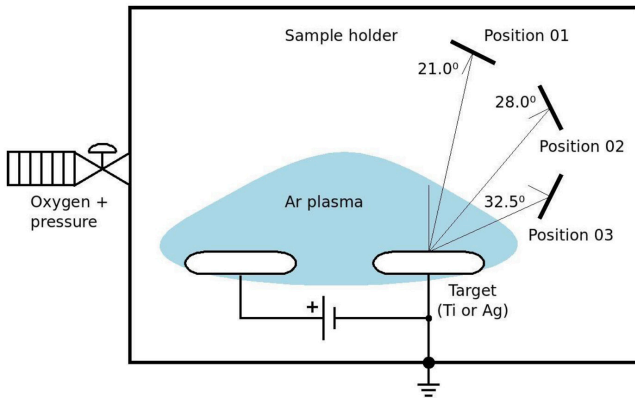
Fig. 1. Schematic representation of the DC Sputtering equipment.

The optical properties were investigated by spectrophotometry at three different wavelengths (λ = 458, 550 or 660nm) using the approximation of infinite thin homogeneous film with uniform thickness d and complex refractive index $n_c = n + ik$ over transparent substrates with refractive index n_b. The substrate is considered to be perfectly smooth, but thick enough with planes not perfectly parallel so that all the interference effects due to the substrate are destroyed. The system is surrounded by air with refractive index $n_0 = 1$. The transmission T for normal incidence presents peaks and valleys and the envelopes around the maximum T_{M0} and minimum T_{m0} were considered to be continuous functions of λ, where the real part of the complex refractive index n_c can be calculated at any wavelength as in [6]:

$$n = \left[N + \left(N^2 - n_b^2 \right)^{1/2} \right]^{1/2} \qquad (1)$$

where

$$N = 2 n_b \left(\frac{T_{M0} - T_{m0}}{T_{M0} T_{m0}} \right) + \frac{n_b^2 + 1}{2} \qquad (2)$$

The film thickness was obtained from light with two different wavelengths (λ_1 and λ_2) as follows [6]:

$$d = \frac{M \lambda_1 \lambda_2}{2. \left(n_1 \lambda_2 - n_2 \lambda_1 \right)} \qquad (3)$$

where $M = 1$ for consecutive peaks and n_1 and n_2 are the refractive indexes for each wavelength, λ_1 and λ_2, respectively. On the other hand, the imaginary part of the refractive index n_c (or extinction coefficient) can be calculated at any wavelength as

$$k = -\ln(\alpha) \frac{\lambda}{4 \pi d} \qquad (4)$$

where the absorption coefficient α is given by

$$\alpha = \frac{(n+1)(n_b+n)\left[1 - (T_{M0}/T_{m0})^{1/2}\right]}{(n-1)(n_b-n)\left[1 + (T_{M0}/T_{m0})^{1/2}\right]} \qquad (5)$$

Double-cavity Fabry-Perot structures were used to measure the transmittance ratio between *s*- and *p*-polarized light beams. This parameter, used to quantify the polarizing effect on narrow band filters, is directly influenced by the birefringence properties of the titania thin films. A MATLAB toolbox to solve the classical optical equations [5] was used to design a narrow band filter centered at 400 and 700nm for the structure [Ag(40nm) / TiO$_2$(160nm) / Ag(80nm) / TiO$_2$(164nm) / Ag(40nm)] shown in the figure 2. Following, figure 3 shows the simulated transmission intensities T_p and T_s for *s*- and *p*-polarized light beams, respectively, having adopted refractive index for *s*-polarization n_s = 2.3977 (λ = 550nm) and refractive index for *p*-polarization n_p = 2.4279 (λ = 550nm) and $k_s = k_p = 0.02$ as measured by spectrophotometry according with the procedure reported by Swanepoel [6] for TiO$_2$ films deposited by DC sputtering onto glass with an inclination angle of 21° (see figure 1).
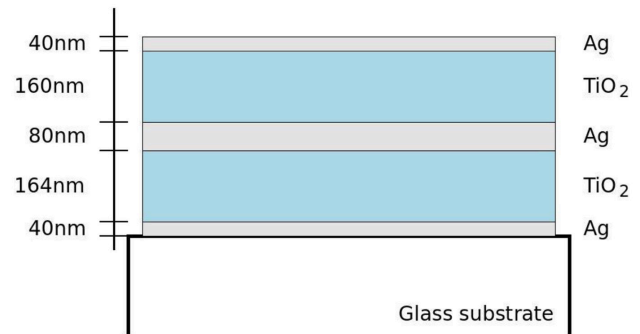
Fig. 2 Fabry-Perot thin-films structure.
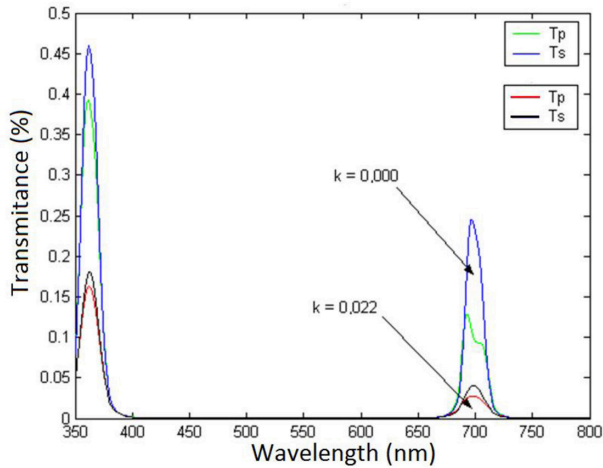
Fig. 3 Transmission intensities T_p and T_s for s- and p-polarized light beams as a function of the wavelength (k = 0.000 and k = 0.022).

Based on the same parameters for the double cavity structure (fig. 2), the imaginary part of the complex refractive index (extinction coefficient) of TiO_2 was simulated for 0.000 and 0.022 in order to predict its influence on the transmittance (%) as shown in figure 3. As a result, the higher the extinction coefficient, the lower the transmittance ratio (T_s/T_p). As shown in equation (4), the absorption and extinction coefficients are correlated. On the other hand, as reported in literature, higher absorption coefficient may be caused by lack of oxygen during the titanium-oxide deposition [8], so leaving an excess of metal.

RBS (Rutherford Backscattering Spectrometry) was used to obtain film composition using a probing beam of $^2He^+$ ions with an energy of 2.2MeV under normal incidence and with a scattering angle of 170°. Aerial concentration of a given element is proportional to the area under the element signal in the RBS spectrum [9]. Based on this fact, the stoichiometric composition of titanium oxide (TiO_x) can be obtained as the ratio between the aerial concentrations of oxygen (N_{Po}) and titanium (N_{PTi}) as follows [9]:

$$x = \frac{N_{Po}}{N_{PTi}} = \frac{A_o \sigma_{Ti}}{A_{Ti} \sigma_o} \qquad (6)$$

where A_o is the area under the oxygen signal, A_{Ti} is the area under the titanium signal, σ_o is the differential cross section for oxygen and σ_{Ti} is the differential cross section for titanium [9]. Besides calculating film thickness by equation (3), it was specifically obtained from RBS spectra of the double-cavity Fabry-Perot structure as the ratio between aerial (N_{PTiOx}) and volumetric concentration (N_{VTiOx}). SIMNRA program [10] was employed to adjust the simulated RBS spectra to the experimental ones in order to precisely extract the aerial concentrations and obtain the film stoichiometry according with the equation (6).

III. Results and Discussion

Table 1 shows the optical properties (d, n_s, n_p, Δn, k_s and k_p) and the stoichiometric parameter (x of the TiO_x) as obtained after DC sputtering onto glass sheets tilted at 21.0°, 28.0° and 32.5° (see figure 1). k_s and k_p are the extinction factors obtained from equation (4) substituting n_s and n_p, respectively. It is observed similar film thickness for the three inclination angles after simultaneous deposition, but nearly-stoichiometric titania (TiO_2) was only obtained for 21°. In this case, it was observed the highest birefringence of 0.0302. In addition, it was observed similar extinction coefficients (k_s and k_p) for all inclination angles.

Table 1 – Optical properties (d, n_p, n_s, Δn, k_p and k_s) and the stoichiometric parameter (x) as obtained after DC sputtering onto glass sheets tilted at 21.0º, 28.0º and 32.5º.

Run	Angle	d(nm)	n_p	n_s	Δn	k_p	k_s	x of TiO_x
	21.0	121.2	2.4279	2.3977	**0.0302**	0.0222	0.0217	1.89
01	28.0	121.5	2.3934	2.3835	0.0099	0.0171	0.0173	1.76
	32.5	119.5	2.3850	2.3767	0.0084	0.0183	0.0182	1.76
	21.0	190.5	2.4762	2.4484	**0.0278**	0.0162	0.0133	1.89
02	28.0	184.6	2.4540	2.4445	0.0095	0.0123	0.0121	1.76
	32.5	182.8	2.4739	2.4574	0.0165	0.0155	0.0132	1.76

Also, in Table 1, it is pointed out lower Δn, lower x and higher k for inclination angles of 28.0° and 32.5°. This may be understood considering a possible non-uniform oxygen distribution at these inclination angles during DC sputtering due to the proximity of the Argon Plasma (see the distances in figure 1). On the other hand, the high extinction coefficients (k) for 28.0° and 32.5° implies in a high film absorption and, as predicted from figure 3 (for $k > 0.022$), it may result in an undetectable transmittance ratio (T_s/T_p) for the double cavity Fabry-Perot Structure.

Table 2 shows the optical parameters n_s, n_p and Δn for

Table 2 – Optical parameters n_p, n_s, Δn, k_p, α_p, k_s and α_s for three different wavelengths (458, 550 and 660nm) for the 159.9 nm-thick film deposited at an inclination angle of 21.0º (near titania stoichiometry).

Run	λ(nm)	n_p	n_s	Δn	k_p	α_p	k_s	α_s
	458	2.4503	2.4190	0.0313	0.0177	0.9428	0.0176	0.9432
01	550	2.4279	2.3977	**0.0302**	0.0222	0.9401	0.0217	0.9404
	660	2.4085	2.3793	0.0292	0.0266	0.9405	0.0258	0.9422
	458	2.4708	2.4373	0.0335	0.0188	0.9064	0.0157	0.9212
02	550	2.4762	2.4484	**0.0278**	0.0162	0.9319	0.0133	0.9438
	660	2.4782	2.4547	0.0235	0.0129	0.9543	0.0104	0.9630

three different wavelengths (458, 550 and 660nm) for the 159.9nm-thick film deposited at an inclination angle of 21° (near titania stoichiometry). It is observed a slight decreases of n_p, n_s and Δn when λ is increased. These observations are similar to that already reported for evaporated TiO_2 films.
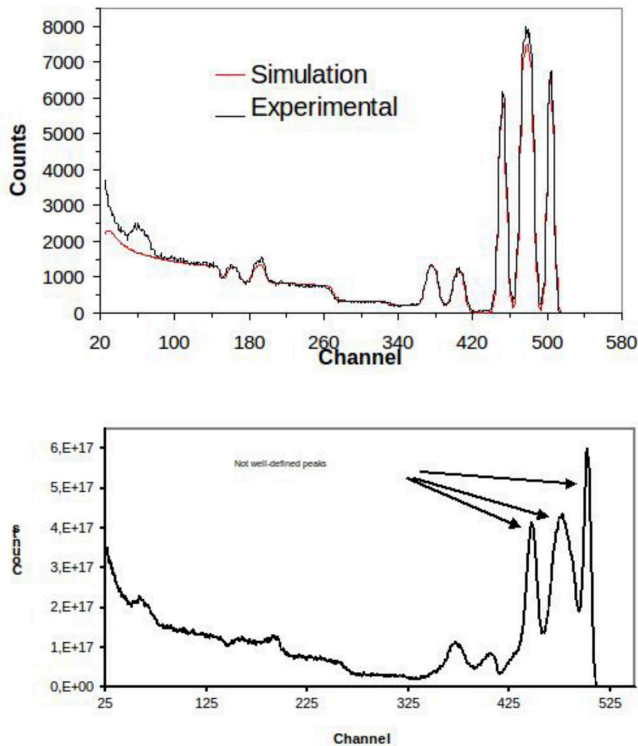
Fig. 4 Typical RBS spectrum for a Ag (40nm) / TiO$_2$ (160nm) / Ag (40nm) / TiO$_2$ (164nm) / Ag (40nm) Fabry-Perot structure superimposed to the corresponding SIMNRA simulated curve deposited at inclination angles of (a) 21° and (b) 28°.

Figures 4a and 4b show typical RBS spectra of double-cavity Fabry-Perot structures for inclination angles of 21° and 28°, respectively. For both inclination angles, it is noteworthy the good fitting between the measured and simulated curves, showing the presence of the Ag, Ti and O signals. In addition, the near titania stoichiometry (TiO$_{1.9}$) was confirmed for inclination angle of 21° and thicknesses for all layers were extracted from SIMNRA simulation whose fitting is presented in the figure 4a. As a result, the structure stands for [Ag(40nm) / TiO$_2$(160nm) / Ag(80nm) / TiO$_2$ (164nm) / Ag(40nm)]. On the other hand, for inclination angle of 28° (figure 4b), the measured signals for Ag, Ti and O presented broader and less defined peaks indicating that an inter-diffusion of Ag into TiO$_x$ occurred and, as consequence, the Ag/TiO$_x$ interface is not well defined compared to the RBS spectrum in figure 4a for the inclination angle of 21°. A similar behavior was also observed for the position with inclination angle of 32.5° and is attributed to local Ar-plasma bombardment. SIMNRA simulation allowed one to estimate an average inter-diffusion length of 50nm between Ag and TiO$_x$ in the figure 4b. So, the Ag/TiO$_x$ inter-diffusion that occurs for inclination angles of 28.0° and 32.5° can be indirectly correlated with the results in Table 1. As already mentioned, a possible non-uniform oxygen distribution at 28.0° and 32.5° must be being caused by local non-uniform Ar/O-plasma effect during the film deposition.

As mentioned in the experimental part, two types of double-cavity Fabry-Perot structures were manufactured:

the FP1 and FP2 devices, both fabricated using an inclination angle of 21° during the depositions. Figure 5 shows the Transmittance x Wavelength characteristic for the FP1 device. In this case, the peaks corresponding to the narrow bands were centered at 393nm and 699nm, respectively, and the transmittance ratios were $T_s/T_p = 1.70$ for λ = 699nm and $T_s/T_p = 1.36$ for λ = 393nm. Also, it is noteworthy that the positions of the narrow-band peaks are in good agreement with the previous simulation presented in figure 3 and the transmittance ratios T_s/T_p fitted well for k = 0.022 (1.65 in fig. 3 against 1.73 in fig. 5). Addressing Table 2 again, it is observed that k can vary from 0.0132 to 0.0217 for λ in the range of 458 to 660nm which means an average value of 0.017, thus, close to the simulated one.
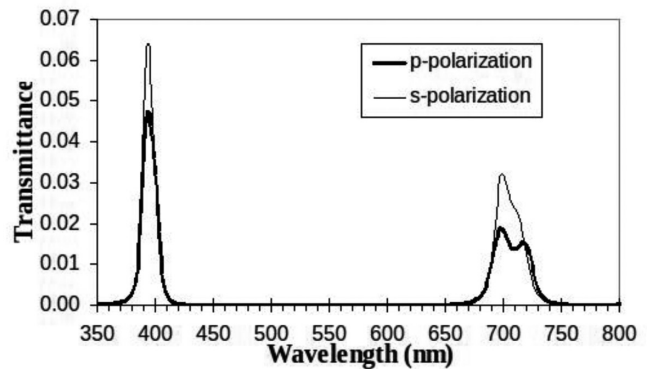
Fig. 5 Transmittance x Wavelength characteristic for the FP1 device. The peaks are centered at 393 and 699nm.

On the other hand, for the FP2 device, figure 6 shows the narrow bands centered at 417nm and 761nm for *p*-polarized light and centered at 420nm and 765nm for *s*-polarization light, this is to say, it occurs a slight shift of the transmittance peaks when "*p*" is changed to "*s*". These measurements are consistent with different optical paths (*n.d*) for *s*- and *p*-polarized lights and are very close to the simulated ones. Therefore, the birefringent characteristics of the near titania stoichiometry (TiO$_{1.9}$) thin films were confirmed with the aid of the FP1 device.
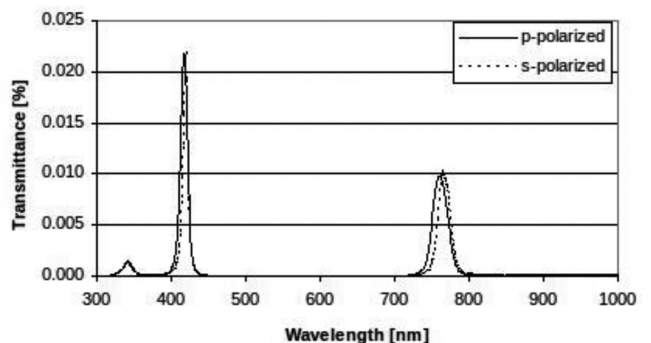
Fig 6 Transmittance x Wavelength characteristic for the FP2 device. The peaks centered at 415 and 770nm.

In addition, for inclination angles of 28° and 32.5°, the transmittance ratios (T_s/T_p) became below the detection limit of the commercial equipment used for spectrophotometry. This result can be understood by the high extinction coefficients that were measured for these conditions. From simulations, $T_s/T_p = 0.000005$ is obtained for k next to 0.07. Therefore, due to high absorption in the film, very low intensities are transmitted for s- or p-polarized light.

Conclusions

It was presented a study related to the birefringence characterization of near-titania-stoichiometry thin films deposited by DC sputtering over tilted glass plates using a titanium target (99.999%) in an oxygen partial pressure of 4×10^{-4} Bar. Film thickness was varied from 60 to 180 nm. Total planar concentration and composition were obtained with the aid of Rutherford Backscattering (RBS) analysis using a 2.2MeV He$^+$ beam at normal incidence and detection at a backscattering angle of 10º. Refractive index and thickness were also obtained by spectrophotometry as a function of the deposition angle and, as a result, the maximum measured birefringence was 0.03. On the other hand, birefringent titania thin films were used in the fabrication of polarizing Fabry-Perot filters, as multilayer structures, having two cavities of titania interposed by silver thin films. A polarizing narrow-band Fabry-Perot filter centered at 400 and 700nm was designed by means of numerical simulations of the multilayer structures using a MATLAB toolbox specially designed to solve the classical optical equations. Figure 4a shows the typical RBS spectrum for a Ag(40nm) / TiO$_2$ (160nm) / Ag(40nm) / TiO$_2$ (164nm) / Ag(40nm) Fabry-Perot structure superimposed on the corresponding SIMNRA simulated curve. The fabricated structure had the transmittance measured for s- and p-polarized light beams, as shown in figure 5. The polarizing characteristics of the filters were changed by sample rotation of 90° for each cavity at a given deposition angle. As a result, for the Fabry-Perot filters, the transmitted light was preferentially polarized (s or p) and allowed one to confirm the birefringent characteristics of the titania thin films.

References

[1] H. Han, X. Zhang and F. Guan, "Computational polarization difference underwater imaging based on image fusion", SPIE Proceedings, vol. 10244, pp. 1, 2017.

[2] Z. Bomzon, V. Kleiner, and E. Hasman, "Space-variant polarization state manipulation with computer-generated subwavelength metal stripe gratings. Optics Communications", vol. 192, pp. 169-181, Jun. 2001.

[3] M.P. Rowe, J.M. Corless, N. Engheta and E.N. Pugh Jr., "Scaning interferometry of sunfish cones. I. Longitudinal variation in single-cone refractive index". Journal of Optical Society of America A, vol. 13, pp. 2141-2150, November 1996.

[4] R.D. Guenther, "Modern Optics", John Wiley, New York, 1990.

[5] I. J. Hodgkinson and Q.H. Wu, "Birefringent thin films and polarizing elements", World Scientific, Singapore, 1997.

[6] R. Swanepoel, "Determination of surface roughness and optical constants of inhomogeneous amorphous silicon films". Journal of Physics E: Scientific Instrumentation, vol. 17, pp. 896-903, February 1984.

[8] A. Dakka, J. Lafait, M. Abd-Lefdil and C. Sella. "Optical study of titanium dioxide thin films prepared by R. F. Sputtering". Journal of Condensed Matter, vol. 2, pp. 153-156, December 1999.

[9] W.K. Chu, J.W. Mayer, M.A. Nicolet, "Backscattering Spectrometry", Academic Press, New York, 1978.

[10] M. Mayer, "SIMRA, a Simulation Program for the Analysis of NRA, RBS and ERDA", Proceedings of the 15th International Conference on the Application of Accelerators in Research and Industry, J.L. Duggan An I.L. Morgan (eds.) American Institute of Physics Conference Proceedings. vol. 571, pp. 475 1999.